RSC Advances

ROYAL SOCIETY OF CHEMISTRY

www.rsc.org/advances

Journal Name RSC Advances Dynamic Article Links ►

Cite this: DOI: 10.1039/c0xx00000x

www.rsc.org/xxxxxx

ARTICLE TYPE

High aspect ratio TiO_2 nanowires tailored in concentrated HCl hydrothermal condition for photoelectrochemical water splitting

Jinzhan Su*, Liejin Guo

Received (in XXX, XXX) Xth XXXXXXXXX 20XX, Accepted Xth XXXXXXXXX 20XX
DOI: 10.1039/b000000x

TiO_2 nanowire/nanorod array grown on FTO substrate by hydrothermal reaction have attracted great attentions because of their favorable application in DSSC and quantum dot solar cells. In this paper, discrete vertically aligned TiO_2 nanowire arrays with their length as long as 7.2 μm and their diameter less than 100 nm were successfully synthesized on FTO substrate by hydrothermal method. The influence of hydrothermal precursor composition on the morphologies of the grown wires was investigated. The photoelectrochemical water splitting performance for nanowires with different lengths were studied. The best photoelectrochemical performance was observed for the longest array without compact layer. The growth mechanism in the concentrated HCl was also proposed. The TiO_2 nanowire array developed in this paper provides an optimal structure for those energy harvesting application requiring long and discrete nanowires as electron collector.

1. Introduction

Nanostructural titanium oxide based material (e.g. nanowires, nanotube or nanoporous structure) has gained intense attention due to their unique chemical and physical properties.[1] The utilization of such advanced nanostructure on dye-sensitized solar cells,[2] quantum-dot solar cells,[3] photoelectrochemical water splitting,[4] gas sensor[5] and batteries[6] boost the development of nanostructural materials. Compared to nanoparticles, one dimensional nanorod/nanowire/nanotube arrays provide un-interrupted electrical pathways and promote the accessibility of holes to the electrolyte, as a result improving the electron transfer rate[7] and efficiency in energy harvest systems. Numerous semiconductor materials in one dimensional form have been investigated for energy conversion.[8]

TiO_2 is the first discovered semiconductor material for solar fuel conversion and remain one of the most important candidates because of its excellent chemical stability, photocorrosion resistance, and low cost.[9] Before the reported of hydrothermal synthesized TiO_2 nanowire arrays in 2008,[10,11] most of the reported one-dimensional TiO_2 nanostructures were synthesized in the form of disoriented nanowires/nanotubes or oriented arrays on nontransparent or nonconductive substrates using various synthesis techniques. Disoriented nanowires/nanotube was synthesized by hydrothermal treatment of TiO_2 nanoparticles in NaOH solution,[12] Electrospun,[13] Biotemplating[14] AAO(anodic alumina oxide)[15] and ZnO nanorod template.[16]

TiO_2 nanowire arrays on different substrates were also reported such as Ti foil treated in concentrated NaOH aqueous solution[17] or annealed in oxygen flow[18] or an argon stream with acetone.[19] Oriented needlelike titanium dioxide (TiO_2)[20] and TiO_2 nanorod arrays[21] were grown on glass substrate with $TiCl_3$ and NaCl aqueous solution. Short TiO_2 nanorod arrays on transparent conductive substrates were synthesized via the hydrolysis of $TiCl_4$ under the co-existence of amino acid catalysts.[22] Some methods like dc reactive magnetron sputtering,[23] pulsed laser deposition (PLD),[24] CVD[25] were also adopted to deposited TiO_2 nanorods. Hierarchically TiO_2 nanoarrays was synthesized by acid vapor oxidation of metallic Ti film.[26] Another type of hierarchically TiO_2 was reported by Chen[27] who grew TiO_2 nanowires on electrospun titania fiber by hydrothermal treatment in $Ti(OBu)_4$–HCl–H_2O solution.

It was until 2008 that high quality oriented single-crystalline TiO_2 nanowires on substrates of transparent conducting (TCO) glass were reported by Feng[10] and Liu[11] by hydrothermal method. Their techniques were then used by many groups to growth TiO_2 nanowire/nanorod for DSSC[28], quantum dot[29] and perovskite[30] solar cells While most reports use the same synthesis strategy without optimization. Tuning the nanorod structures such as the nanorod thickness, length, and density are very good candidates for further improving the efficiency. For example, hierarchical TiO_2[31,32] with enhanced photovoltaic performance have been reported. While decreasing the diameter and increasing the length remain a promising way to further improve the light harvesting and conversion performance of TiO_2 nanowires/nanorods. The TiO_2 nanorod reported by Liu[11] possess a relatively large diameter of 100nm and short length. The diameter of TiO_2 nanowires reported by Feng[10] is thinner but compactly packed as nanowire bundles. Comparing these TiO_2 nanorods, discrete nanorods with longer length and thinner diameter can derive to better infiltration of both the light absorber and the hole transporting material.

In this paper we report growth of well aligned discrete nanowire arrays on FTO substrate with modified method based on Feng's technique. The nanowire arrays can be grown up to

μm while avoiding grown into compact bundles. The influence of different composition and growth mechanism were discussed. To demonstrate their application in solar water splitting, the TiO_2 nanowires with different lengths were used as photoanodes. The knowledge gained from this work will help understand the growth mechanism and provide strategy to tailoring the nanowire morphology. This study demonstrate synthesis of TiO_2 nanowire arrays with a long length and thin diameter, which are promising applications in photoelectrochemical water splitting, dye-sensitized solar cells and quantum-dot solar cells.

2. Experimental

2.1 Preparation of TiO_2 nanoiwre arrays

The synthesis of the TiO_2 nanowire arrays was performed by hydrothermal method. In a typical procedure, an anatase TiO_2 seed layer was initially deposited on FTO coated glass(TEC 8, 8 Ω per square) by spincoating using a solution prepared by dissolving 1.7 ml Ti butoxide and 0.2 g poly(vinyl alcohol) (PVA) in 5 ml deionized water and 5ml acetic acid, followed by 500 °C annealing for 2 h in air. The seed layer coated substrate was then placed within a Teflon lined autoclave (23 ml), containing 2ml of titanium tetrachloride (1 M in toluene) and 8 ml of hydrochloric acid (37 wt%). The concentration of $TiCl_4$ was further adjusted by adding certain amount of $TiCl_4$ (Sigma, 99%) into the precursor. The autoclave was then sealed and placed in an oven at 170 °C for 48 h. The substrate was then rinsed with ethanol and dried in a nitrogen stream. All the TiO_2 nanowire arrays were annealed at 500 °C for 0.5 h in air.

2.2 Structural and photoelectrochemical characterization

X-ray diffraction (XRD) patterns were obtained on a PANalytical X'pert MPD Pro X-ray diffractometer using Ni- filtered Cu Kα irradiation (Wavelength 1.5406 Å) to determine the structure and phase of the samples. The sample morphology was observed by a JEOL JSM-6700FE scanning electron microscope and a JEOL JEM 2100 transmission electron microscope (TEM). To prepare sample for TEM measurement, the nanorods were scratched off the substrate and dispersed in ethanol assisted by ultrasonication. A drop of the dispersion was put on a holey carbon film on a copper TEM grid and dry with an infrared lamp. X-ray photoelectron spectroscopy (XPS) data were obtained on a KRATOS AXIS-ULTRA DLD instrument with a monochromatized Al Kα line source (150 W). All binding energies were referenced to the C 1s peak at 284.6 eV. Photoluminescence emission spectra were measured using a fluorescence spectrophotometer (QM-4, PTI). Linear sweep voltammetry and incident photon-to-current conversion efficiency (IPCE) were conducted using a two-electrode setup, platinum foil as counter-electrode and 0.5 M Na_2SO_4 aqueous solution as electrolyte. A scanning potentiostat (CH Instruments, model CHI 600C) was used to measure photocurrents at a scan rate of 25 mV/s and impedance spectra at 0.6 V vs. Ag/AgCl. The light source was a 150 W xenon lamp (Spectra Physics) with AM 1.5 filter (Oriel). The light intensity was set equivalent to global AM 1.5 illumination at 100 mW/cm^2 using a NREL calibrated crystalline silicon solar cell. IPCE measurements were performed using a 300 W xenon lamp (Spectra Physics), integrated with a parabolic reflector, passing through an AM 1.5 filter and computer controlled monochromator with an Oriel calibrated silicon photodiode used for detection.

3. Results and discussion

Well-aligned TiO_2 nanowires were grown vertically on FTO substrate by modified hydrothermal deposition based on Feng's report,[10] as described in the experimental section. Instead of densely packed nanowire array, discrete nanowire arrays were grown by adjusting the composition of hydrothermal precursor. Figure 1a-d shows the nanowire arrays grown with 0 ml, 0.22 ml, 0.44 ml and 0.66 ml $TiCl_4$ (99 wt%) added, respectively. While the amount of $TiCl_4$ toluene solution (1M) added into the precursor, temperature and reaction time were kept as described in the experimental section. The left-sided insets are top views and enlarged images. It was found that the wire length could be well controlled by varying the amount of $TiCl_4$ in the precursor. The lengths of the nanowires were measured to be about 0.7 μm, 2.9 μm, 7.2 μm and 26 μm, respectively. As shown in the insets in Figure 1a-d, when the $TiCl_4$ amount in the precursor increased, the diameters didn't change much until 0.66 ml $TiCl_4$ was added. For the samples without addition of $TiCl_4$, the diameters ranged from 21 nm to 65 nm with diameter of most wires at 42 nm. With the volume of $TiCl_4$ precursor increased to 0.22 ml and 0.44 ml, the diameter range increased slightly to that from 23 nm to 101 nm. While with 0.66 ml $TiCl_4$ added, the diameters of the wires increased to values between 43 nm and 220 nm. In addition, a dense packed nanorod layer(basal region, with thickness of 16 μm) was grown before the growth of discrete nanowires (top region, 10 μm) as shown in figure 1(d). To the best of our knowledge, the nanowire arrays with length as long as 7.2 μm and their diameter less than 100 nm possess the highest aspect ratio among the reported TiO_2 wire arrays. It was found that the longest discrete TiO_2 wire can be grown is 10 μm in length, further increase of $TiCl_4$ added will lead to formation of undesired compact layer. The digital pictures for the nanowires with different lengths are shown in figure S1.

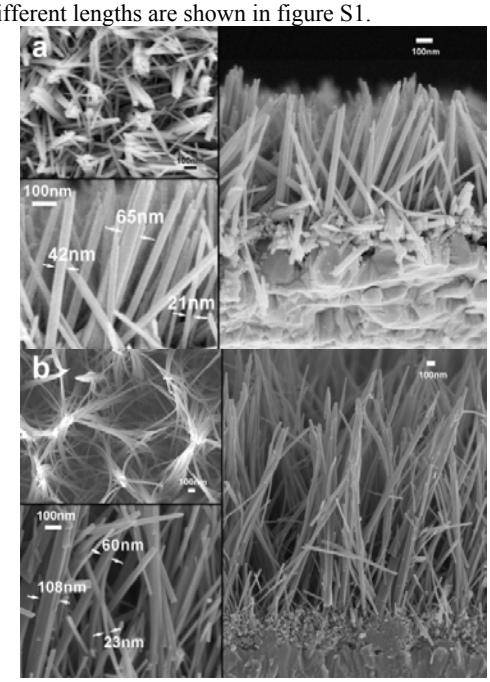

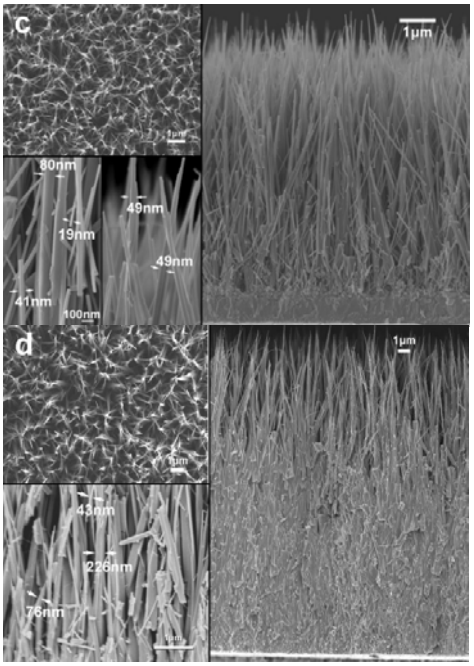

Fig. 1 SEM images of TiO_2 nanowires grown on FTO substrate with different amount of $TiCl_4$ added. (a)0 ml (b)0.22 ml (c)0.44 ml (d)0.66 ml. The upper insets show the top view of samples and the lower inset show the enlarged images of cross section. Note: there is a base amount of $TiCl_4$ added by 2 ml of $TiCl_4$ toluene solution(1M).

To identify the structure of the as-grown array, XRD measurements were conducted in powder mode. Figure 2 shows XRD patterns of the TiO_2 nanowire arrays grown with different amount of $TiCl_4$ added in to the precursor. With the exception of the reflection from the substrate (FTO, marked with star symbols), the characteristic peaks in XRD can be well indexed as rutile TiO_2 (JCPDS: 004-0551). In addition, the intensity of (002) peaks increases significantly with respect to increasing film thickness, revealing a nanowire growth direction along [001].

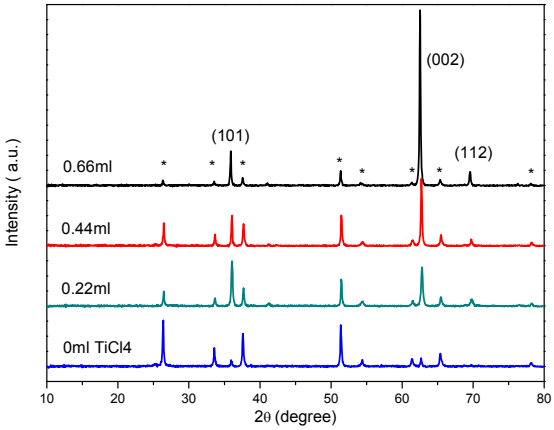

Fig. 2 XRD patterns of TiO_2 nanowires grown on FTO substrate with different amount of $TiCl_4$ added. (a)0 ml (b)0.22 ml (c)0.44 ml (d)0.66 ml. Peaks marked with * are peaks of FTO.

More details about microstructures of the as-prepared nanowires were obtained by TEM analysis, as shown in figure 3(a). The TEM analysis reveals that the as synthesized nanowires are high aspect ratio with diameter from a few nanometers to hundred nanometers. Figure 3(b) shows the high-resolution TEM (HRTEM) image of TiO_2 nanowires. Lattice planes are distinctly visible. The lattice spacing of 3.23 Å can be readily assigned to (110) crystal plane of rutile TiO_2. The nanowire is confirmed to be single crystalline with growth direction of [001]. XPS spectra of Ti2p and O1s for the nanowire grown with 0.22 ml $TiCl_4$ added are shown in figure 3(c), (d). A curve-fitting analysis was performed for the O1s spectra by Levenberg-Marquardt curve-fitting method, assuming the superposition of two components' peaks (dashed lines), which can be assigned to the lattice oxygen (529.5 eV) and the surface bridging oxygen (531.2 eV).[33] The atom ratio between the surface bridging oxygen and the lattice oxygen was calculated to be 0.85. The high ratio of surface bridging oxygen could be a result of high surface area of nanowire structure.[33] As shown in Figure S2, only Ti, O and C (for calibration) were found in the XPS survey scan, which indicates that impurity-free TiO_2 nanowires were grown.

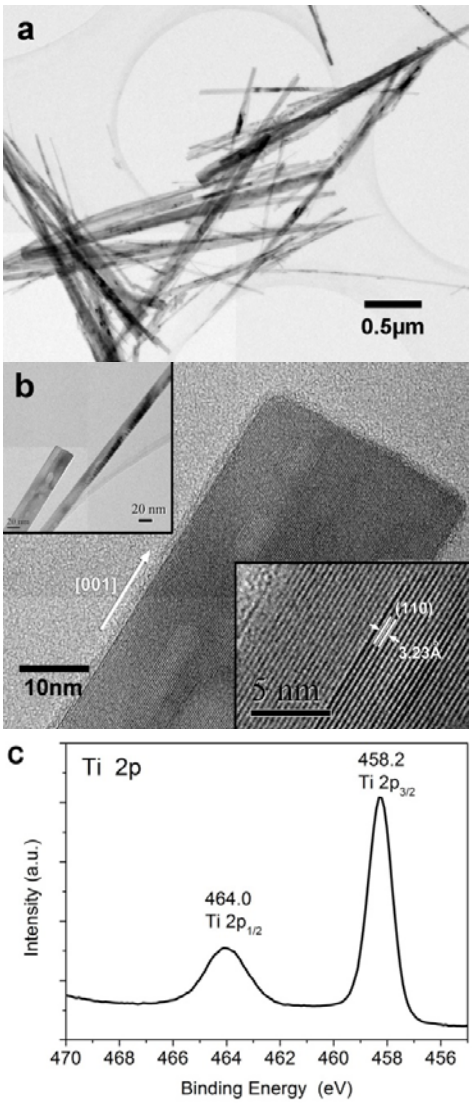

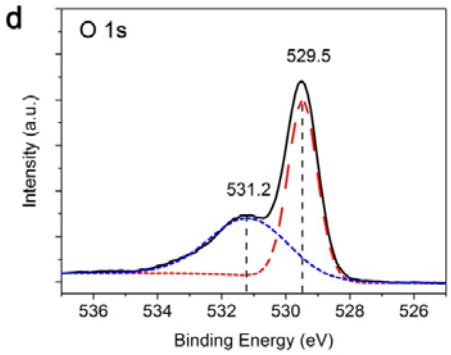

Fig. 3 (a) SEM and (b) High-resolution TEM image and XPS spectra of (c) Ti 2p and (d) O1s for the TiO_2 nanowire grown with 0.22 ml $TiCl_4$ added.

Photoluminescence emission spectra of TiO_2 nanowires with different lengths were measured with excitation wavelength of 337 nm at room temperature. As shown in figure S3, emission bands at 425 nm, bands in the region of 300-430 nm and at 556 nm were observed for all four samples, which can be assigned to three kinds of physical origins: self-trapped excitons localized on TiO_6 octahedra, oxygen vacancies and surface states, respectively.[34,35] It is indicated that oxygen vacancies and surface states existed in the nanowires. The 400 nm band for sample with 0 ml and 0.22 ml $TiCl_4$ added could be from FTO substrate since their thin TiO_2 layer. The intensities of the observed PL bands increased as the amount of $TiCl_4$ added increased from 0 ml to 0.44 ml and then decreased at 0.66 ml. The first increase can be attributed to increase of nanowire array length and their surface area, while for the sample of 0.66 ml, the decrease of emission intensity can be ascribed to the surface area decreased with the diameter of the nanowire increased (as shown in figure 1d).

To get comprehensive understand of photoelectrochemical properties TiO_2 nanowires with high aspect ratio and discrete bundle, current-voltage curves and IPCE measurement were carried for samples with different nanowire length under back illumination (from the substrate side) as shown in figure 4. It was found that photocurrent increased with nanowire length till 7.2 μm length of the nanowires, this can be interpreted that electrons were generated close to back contact of the electrode where electron collection efficiency is high, longer nanowire length gave more photogenerated electrons to transport to back contact. But when the wire length reached 26 μm, with which a compact base was formed, the photocurrent decreased significantly. This can be interpreted as the compact base layer significant increased the hole transport path to the electrolyte as well as the electron transport path to the back contact. So the base layer should be avoid for an efficiency photoelectrochemical application. The dependence of IPCE on wire length has a similar trend for all four samples. For the sample possessing largest wire length of 7.2 μm without compact layer, maximum IPCE values of 47% at 365nm could be seen under potential at 0 V versus Ag/AgCl.

In order to illustrate the charge transport properties of the TiO_2 nanowires, electrochemical impedance spectroscopy (EIS) was carried out in the dark under a bias of 0.6 V vs. Ag/AgCl. Figure S4 depicts the Nyquist plots of nanowires with different lengths. The larger curves for the longer wires in the Nyquist plots are ascribed to a larger charge-transfer resistance related to recombination of electrons at the TiO_2/electrolyte interface.[36] Moreover, the sample with 0.44 ml $TiCl_4$ added possessed much longer wire than that with 0.22 ml but exhibit a close charge-transfer resistance, which is agreement with the highest photocurrent achieved in sample with 0.44 ml $TiCl_4$ added and possible due to the fewer grain boundaries and surface defects existing in the sample with 0.44 ml $TiCl_4$ added.[31]

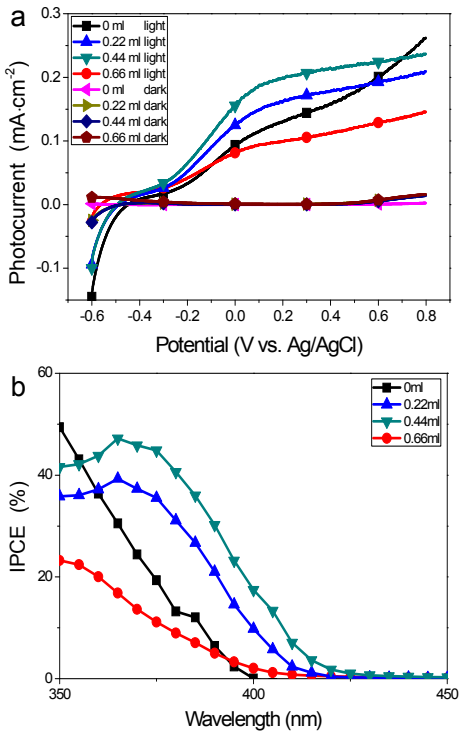

Fig. 4 (a) I-V photoelectrochemical response and (b) incident photon-to-current efficiency (IPCE) for TiO_2 nanowire arrays with different lengths. The IPCE measurements were performed under potential at 0 V versus Ag/AgCl. The electrolyte for both I-V and IPCE tests were 0.5M Na_2SO_4.

To achieve better growth control and further understand the growth mechanism, different growth parameters in strong acid medium to growth TiO_2 nanowire/nanorod with various morphologies were investigated.

Effect of amount of Ti source

When using Feng's method,[10] TiO_2 thin nanowire with diameter of 10 to 35 nm and length up to 5μm were grown in toluene medium with both Ti butoxide and $TiCl_4$ (1M in toluene) as Ti source. To prepare the precursor, 1 ml hydrochloric acid (37 wt%) and certain amount of both Ti butoxide and $TiCl_4$(1M in toluene) were added, corresponding amount of toluene was added to keep the total volume of precursor as 15 ml. It was found that the concentration of Ti source determined the thickness in a linear manner. We used same volume for both Ti butoxide and $TiCl_4$(1M in toluene) added and adjusted to 0.5 ml, 1 ml or 2 ml, TiO_2 nanowire arrays with thickness of 1.4, 2.7 and 5.1 μm, respectively, were grown as shown in figure S5. The basal regions of the nanowires grown by the method were found to bunch together, which may prevent electrolyte penetration and dye molecule absorption for DSSC or quantum dot loading for quantum dot solar cells. That should be why in Feng's research,

the shortest nanowire exhibit best performance regarding to DSSC application.[10]

As the concentration of Ti source played an important role in wire growth, we further adjust the amount ratio of Ti butoxide to $TiCl_4$ (1 M in toluene) added while keeping the hydrochloric acid (37 wt%) unchanged and total volume at 15 ml by adding toluene. For rich $TiCl_4$ precursor, with 4 ml of $TiCl_4$ (1M in toluene) and 1ml of Ti butoxide added (1 ml hydrochloric acid (37 wt%) and certain amount toluene were added to keep total volume of precursor as 15 ml), nanowire arrays with discrete wire tips was grown (figure S6(a)). The tips of discrete TiO_2 gather together into a bunch, this apparent deformation is most probably introduced during the air-drying of the specimens.[37] While using rich Ti butoxide precursor, with 4 ml of Ti butoxide and 1ml of $TiCl_4$(1M in toluene) added, a compact TiO_2 layer instead of nanowire arrays was grown as shown in figure S6(b).

It was believed that high concentration of Ti source lead to formation of dense packed nanowire arrays. At the start of the reaction, Ti concentration is high in the precursor, dense packed nanowires were grown. As reaction went on, the concentration of Ti dropped and discrete nanowires started to grow as the tip of wires. Moreover, the Cl^- ions contribute the formation of discrete nanowires. That's why keeping Ti butoxide amount unchanged at 1ml while adding 4ml instead of 1ml of $TiCl_4$ (1 M in toluene) into the precursor, the tip region of the wires turn to discrete arrays (figure S6(a)). Cl^- was believed to be the structure director for TiO_2 nanowire growth[10,11] and can be selectively adsorbed onto the (110) crystal plane[38] suppressing further growth of this plane, and resulting in anisotropic growth in the [001] direction.

To further check the influence of the ratio of Ti butoxide to $TiCl_4$ on the morphology of TiO_2 nanorods, a controlled experiment is carried out by keeping the amount of $TiCl_4$ (1 M in toluene) unchanged at 4 ml and decreasing the amount of Ti butoxide from 1ml to 0.1ml and the results are illustrated in figure S7. It is found that the thickness of the dense packed basal regions decrease while thickness of the discrete regions keeps unchanged at approximately 600-800 nm.

Effect of growth medium

The growth medium is also important to the evolution of morphology. Nanowire can be grown in both toluene and HCl medium. When 2 ml $TiCl_4$(1 M in toluene) and 4 ml HCl (6 M) were added into 10 ml toluene, the toluene and the HCl aqueous solution separated and formed two layers as the two solutions are immiscible, e.g. the lighter toluene in the upper layer and the heavier HCl aqueous solution in the lower layer. The $TiCl_4$ is more soluble in HCl solution so after ultrasonication the $TiCl_4$ will transfer from toluene to HCl solution and the upper layer turn from red color to colorless. A substrate was vertically placed in the autoclave, with its upper part and lower part immersed in different medium as shown in figure 5. After reaction at 170 ^oC for 4 h, nanowires with different morphologies were grown on these two different parts of the substrate. The nanowire grown in toluene is discrete nanowire with diameter of 40 nm and length of 700 nm, while the nanowire grown in HCl is also discrete nanowire with diameter of 100 nm and a longer length of 3600 nm.

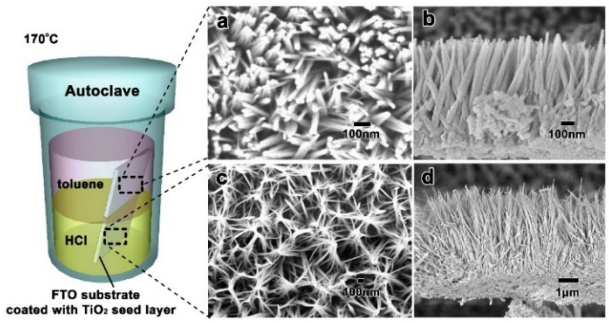

Fig. 5 Top view and cross section veiw SEM images of TiO_2 nanowires grown in toluene layer (a), (b) and HCl aqueous solution layer (c), (d).

The reason why longer nanowires were grown in HCl aqueous solution is that Ti concentration is higher in this medium than that in toluene. When sonicating the mixure of 2 ml $TiCl_4$(1M in toluene) and 4 ml HCl (6M), the red-colored toluene will turn to colorless and HCl turn to milky white because most of the Ti source transfer from toluene to HCl solution.

It was found that when take 37 wt% HCl (12 M) aqueous solution as reaction medium and $TiCl_4$ or Ti butoxide as Ti precursor, no hydrolysis occurred. But when the molarity of HCl solution was reduced to 6 M, TiO_2 nanorod arrays can be grown directly in FTO substrate, this is the case reported by Liu.[11] When 2 ml $TiCl_4$(1 M in toluene) was added into 8 ml 37 wt% HCl (12 M) aqueous solution to be used as precursor, discrete nanowires were grown on TiO_2 seed layer coated substrate and the lengths increased with time. As shown in Figure S8, nanowires with lengths about 100 nm, 930 nm and 2230 nm were grown for 24 h, 48h and 36 h respectively. It should be noted that no nanowire were grown in bare FTO substrate, which is different from the cases that using HCl (6 M) or toluene[10] as precursor. And we increased the concentration of $TiCl_4$ by adding 0 ml, 0.22 ml 0.44 ml or 0.66 ml pure $TiCl_4$ (99%) instead of $TiCl_4$(1M in toluene) and keep volume of toluene at 2 ml, the length of deposited nanowire increased, This is the case discussed in previous section and the optimal nanowire arrays with length of 7.2 μm was obtained with 0.44 ml $TiCl_4$ (99%) added. It is interesting that without toluene, no TiO_2 nanowire were grown in 37 wt% HCl. Thus toluene should play an important role in $TiCl_4$ hydrolysis in HCl with extremely low pH, this will be discussed later in this paper. It should be noted that with this high concentrated HCl precursor, there is no precipitation in the autoclave but only TiO_2 nanowires grow on the substrate and the precursor can be reused for further growth of TiO_2 nanowires. This method is highly efficient in Ti source usage and very suitable for industrial application.

Growth mechanism

In rutile, TiO_6 octahedrons link with each other by sharing two edges along the c axis to construct chains, and then the chains were connected with corner shared bonding.[39] While the anatase TiO_2 framework is constructed by sharing four edges of the TiO_6 octahedron (or face-shared connection). There are more edge-shared bondings in the anatase structure than in the rutile structure (Figure 9). To form edge-shared bonds in anatase structure, more dehydration reactions between titania complexes

must occur simultaneously, which is less likely at high acidic concentrations. Thus, high acidic solution appears preferable for synthesizing rutile and basic solution for anatase phase.[40]

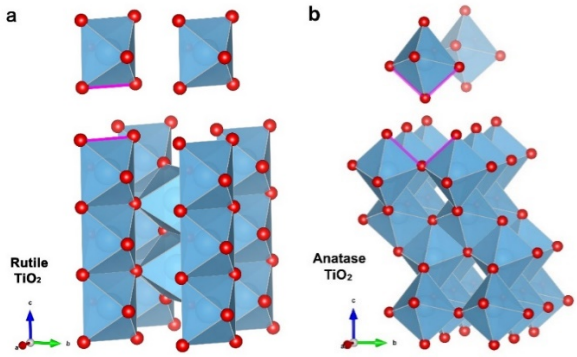

Fig. 6 Crystal structures of (a) rutile and (b) anatase TiO_2. The bond edges (marked with bold line) represent edge-shared bonding, number of which is larger in the anatase structure than in the rutile structure.

According to Nicholls,[41] the titanium(IV) ion was kept in solution as anionic complexes of type $[Ti(OH)Cl_5]^{2-}$ and/or $[TiCl_6]^{2-}$ in HCl aqueous solution where Cl^- coordinated to the titanium. It was considered[39,42] that the Ti(IV) complex ion has the formula $[Ti(OH)_nCl_m]^{2-}$ (H_2O could be a ligand too), where $n + m = 6$, and n and m are determined by the acidity and concentration of Cl^- ion in feedstock. Even though the ligand field strength of OH group is larger than that of Cl^- ion, a higher acidity or $[Cl^-]$ will give a bigger m. The linking between $[TiO_6]$ units during the TiO_2 nanowires growth is considered to be carried out by dehydration reactions (i.e., oxolation) between OH ligands in $[Ti(OH)_nCl_m]^{2-}$ complex ions. When the acidity in feedstock is higher, the number of OH ligand in $[Ti(OH)_nCl_m]^{2-}$ is smaller, the growth of TiO_2 nanowires is suppressed. In concentrated HCl (37 wt%, 12 M), the Ti(IV) complex is the form of $[TiCl_6]^{2-}$ which is not favorable for TiO_2 growth, as Cl^- retard linking of $[TiO_6]$ units. When decreasing the acidity, the concentration of OH^- increased and $[Ti(OH)_nCl_m]^{2-}$(n>0) was formed. Growth of TiO_2 became favorable by dehydration OH ligands in $[Ti(OH)_nCl_m]^{2-}$ complex. As mentioned above, toluene plays an important role in $TiCl_4$ hydrolysis in HCl with extremely low pH. With addition of toluene, hydrolysis of $TiCl_4$ became possible in 37 wt% HCl (12 M) and TiO_2 wires were grown on seed layer coated substrate. This can be explained as follows. Arenes, such as $C_6(CH_3)_6$ can react with Ti(IV) ion to give the piano-stool complexes $[Ti(C_6Me_6)Cl_3]^+$.[43] Similar behavior is observed in case of toluene, in extremely low pH HCl, $[TiCl_6]^{2-}$ can react with toluene to form the complex $[Ti(C_6H_5CH_3)Cl_5]^-$.

$$TiCl_6^{2-} + C_6H_5CH_3 \leftrightarrow \left[Ti\left(C_6H_5CH_3\right)Cl_5\right]^- + Cl^- \quad (1)$$

The replacement of Cl ion with $C_6H_5CH_3$ may further transform to $[Ti(OH)_nCl_m]^{2-}$ and as a result promote the linking of $[TiO_6]$ units, making the growth of TiO_2 become possible in high concentrated HCl solution.

4. Conclusions

In summary, discrete vertically aligned TiO_2 nanowire arrays with their length as long as 7.2 μm and their diameter less than 100 nm were successfully synthesized on FTO substrate by hydrothermal deposition. The TiO_2 nanowires with different lengths were used as photoanodes to investigate their photoelectrochemical properties. The nanowire arrays with length of 7.2 μm synthesized in concentrated HCl (37 wt%) aqueous solution showed the best performance. The influence of hydrothermal precursor composition on the morphologies of the grown wires was investigated in detail. The concentrated HCl is found essential for growth of discrete long nanowire arrays. The growth mechanism of nanowires in concentrated HCl aqueous solution was discussed and it is found that hydrothermal growth of TiO_2 in concentrated HCl became possible with existence of toluene in the precursor and seed layer on the substrate. The results provide an optimal structure for energy harvesting application and insights into growth mechanisms of high aspect ratio TiO_2 nanowires in concentrated HCl aqueous solution.

Acknowledgments

We gratefully acknowledge the financial support from the National Natural Science Foundation of China (No.51202186).

*Corresponding author: Dr. J. Su.
International Research Center for Renewable Energy, State Key Laboratory of Multiphase Flow in Power Engineering, Xi'an Jiaotong University, Shaanxi 710049, P. R. China.
E-mail: j.su@mail.xjtu.edu.cn.

† Electronic Supplementary Information (ESI) available: Fig. S1-S8 include infromation for digital photo of the samples, SEM images of TiO_2 nanowires synthesized using different precursor composition or reaction time. See DOI: 10.1039/b000000x/

References

1 X. Wang, Z. Li, J. Shi and Y. Yu, *Chem. Rev.*, 2014.
2 M. Law, L. E. Greene, J. C. Johnson, R. Saykally and P. Yang, *Nat. Mater.*, 2005, **4**, 455.
3 H.-S. Kim, J.-W. Lee, N. Yantara, P. P. Boix, S. A. Kulkarni, S. Mhaisalkar, M. Grätzel and N.-G. Park, *Nano Lett.*, 2013, **13**, 2412.
4 S. Shen and S. S. Mao, *Nanophotonics*, 2012, **1**, 31.
5 Y.-C. Huang, F.-S. Tsai and S.-J. Wang, *Jpn. J. Appl. Phys.* 2014, **53**, 06JG02.
6 Z. Jin, M. Yang, G. Wang, J. Wang, Y. Luan, L. Tan and Y. Lu, *Nanotechnology*, 2014, **25**, 395401.
7 W. U. Huynh, J. J. Dittmer and A. P. Alivisatos, *Science*, 2002, **295**, 2425.
8 A. I. Hochbaum and P. Yang, *Chem. Rev.*, 2009, **110**, 527.
9 X. Chen and S. S. Mao, *Chem. Rev.*, 2007, **107**, 2891.
10 X. Feng, K. Shankar, O. K. Varghese, M. Paulose, T. J. Latempa and C. A. Grimes, *Nano Lett.*, 2008, **8**, 3781.
11 B. Liu and E. S. Aydil, *J. Am. Chem. Soc.*, 2009, **131**, 3985.
12 C.-Y. Xu, Q. Zhang, H. Zhang, L. Zhen, J. Tang and L.-C. Qin, *J. Am. Chem. Soc.*, 2005, **127**, 11584.
13 I.-D. Kim, A. Rothschild, B. H. Lee, D. Y. Kim, S. M. Jo and H. L. Tuller, *Nano Lett.*, 2006, **6**, 2009.
14 T. H. Han, H.-S. Moon, J. O. Hwang, S. I. Seok, S. H. Im and S. O. Kim, *Nanotechnology*, 2010, **21**, 185601.
15 Z. Miao, D. Xu, J. Ouyang, G. Guo, X. Zhao and Y. Tang, *Nano Lett.*, 2002, **2**, 717.
16 C. Xu, P. H. Shin, L. Cao, J. Wu and D. Gao, *Chem. Mater.*, 2009, **22**, 143.
17 F. Shao, J. Sun, L. Gao, S. Yang and J. Luo, *J. Phys. Chem. C*, 2010, **115**, 1819.
18 T. K. Sung, J. H. Kang, D. M. Jang, Y. Myung, G. B. Jung, H. S. Kim, C. S. Jung, Y. J. Cho, J. Park and C.-L. Lee, *J. Mater. Chem.*, 2011, **21**, 4553.

19 X. Peng and A. Chen, *J. Mater. Chem.*, 2004, **14**, 2542.
20 S. Yamabi and H. Imai, *Chem. Mater.*, 2002, **14**, 609.
21 E. Hosono, S. Fujihara, K. Kakiuchi and H. Imai, *J. Am. Chem. Soc.*, 2004, **126**, 7790.
22 Y. Hayami, Y. Suzuki, T. Sagawa and S. Yoshikawa, *J. Nanosci. Nanotechno.*, 2010, **10**, 2284.
23 L. Meng, T. Ren and C. Li, *Appl. Surf. Sci.*, 2010, **256**, 3676.
24 F. Sauvage, F. Di Fonzo, A. Li Bassi, C. Casari, V. Russo, G. Divitini, C. Ducati, C. Bottani, P. Comte and M. Graetzel, *Nano Lett.*, 2010, **10**, 2562.
25 J.-C. Lee, T. G. Kim, W. Lee, S.-H. Han and Y.-M. Sung, *Cryst. Growth Des.*, 2009, **9**, 4519.
26 X. Yang, J. Zhuang, X. Li, D. Chen, G. Ouyang, Z. Mao, Y. Han, Z. He, C. Liang and M. Wu, *Acs Nano*, 2009, **3**, 1212.
27 C. Sun, N. Wang, S. Zhou, X. Hu, S. Zhou and P. Chen, *Chem. Commun.*, 2008, 3293.
28 K. Shankar, X. Feng and C. A. Grimes, *Acs Nano*, 2009, **3**, 788.
29 J. H. Bang and P. V. Kamat, *Adv. Funct. Mater.*, 2010, **20**, 1970.
30 Q. Jiang, X. Sheng, Y. Li, X. Feng and T. Xu, *Chem. Commun.*, 2014, **50**, 14720.
31 W.-Q. Wu, B.-X. Lei, H.-S. Rao, Y.-F. Xu, Y.-F. Wang, C.-Y. Su and D.-B. Kuang, *Sci. Rep.*, 2013, **3**, 1892.
32 X. Sheng, D. He, J. Yang, K. Zhu and X. Feng, *Nano Lett.*, 2014, **14**, 1848.
33 E. Tsuji, K.-i. Fukui and A. Imanishi, *J. Phys. Chem. C*, 2014, **118**, 5406.
34 Y. Lei, L. D. Zhang, G. W. Meng, G. H. Li, X. Y. Zhang, C. H. Liang, W. Chen, and S. X. Wang, *Appl. Phys. Lett.*, 2001, **78**, 19.
35 F.-J. Knorr, D. Zhang, and J.-L. McHale, *Langmuir*, 2007, **23**, 8686.
36 F. Fabregat-Santiago, J. Bisquert, G. Garcia-Belmonte, G. Boschloo and A. Hagfeldt, *Sol. Energ. Mat. Sol. C.*, 2005, **87**, 117.
37 Y. Sun, N. George Ndifor-Angwafor, D. Jason Riley and M. N. Ashfold, *Chem. Phys. Lett.*, 2006, **431**, 352.
38 M. Adachi, Y. Murata, J. Takao, J. Jiu, M. Sakamoto and F. Wang, *J. Am. Chem. Soc.*, 2004, **126**, 14943.
39 H. Cheng, J. Ma, Z. Zhao and L. Qi, *Chem. Mater.*, 1995, **7**, 663.
40 J. Xie, X. Wang and Y. Zhou, *J. Mater. Sci. Technol.*, 2012, **28**, 488.
41 D. Nicholls, in *Complexes and First-Row Transition Elements*, The Macmillan Press Ltd., New York, 1974.
42 A. Pottier, C. Chanéac, E. Tronc, L. Mazerolles and J.-P. Jolivet, *J. Mater. Chem.*, 2001, **11**, 1116.
43 F. Calderazzo, I. Ferri, G. Pampaloni and S. Troyanov, *J. Organomet. Chem.*, 1996, **518**, 189.